PNAS
www.pnas.org

Supplementary Information for

(p)ppGpp directly regulates translation initiation during entry into quiescence

Simon Diez, Jaewook Ryu[#], Kelvin Caban[#,†], Ruben L. Gonzalez Jr.[#] and Jonathan Dworkin*
Department of Microbiology and Immunology, College of Physicians and Surgeons, Columbia University, New York, NY 10032; [#]Department of Chemistry, Columbia University, New York, NY 10027, [†]Current address: PTC Therapeutics, South Plainfield, NJ, 07080

*Jonathan Dworkin

Email: jonathan.dworkin@columbia.edu

This PDF file includes:

SI Methods
Figures S1 to S7
Tables S1 to S4
SI References

Supplementary Information

SI Methods

Growth curves

Growth curves were performed in a Tecan Infinite m200 plate reader at 37 ºC with continuous shaking and OD_{600} measurements were made every five minutes. Cultures were grown from single colonies from fresh LB plates grown overnight at 37 ºC. Single colonies were picked into 3 mL of LB and grown at 37 ºC for ~2 hours. Cultures were checked to ensure that they were in exponential phase using an Eppendorf Biophotometer (*B. subtilis* grows exponential until OD_{600} ~1.0 as measured by this spectrophotometer as compared to OD_{600} ~0.3 when measured in the Tecan Infinite M200 plate reader). At a time point during exponential phase (OD_{600} ~ 0.5-1.0 as measured by the Eppendorf Biophotometer which correlates to OD_{600} 0.05-0.30 in the Tecan plate reader) , the *B. subtilis* cultures were diluted to OD_{600} = 0.01 and grown in 96-well Nunclon Delta surface clear plates (Thermo Scientific) with 150 μL per well. All growth curves were done in triplicate and media-only wells were used to subtract background absorbance.

OPP labeling

Click-iT Plus OPP Protein Synthesis Assay Kit (Invitrogen) was used to label cells with OPP following manufacturer's instructions. 450 μL of cells at given time points were transferred to disposable glass tubes. OPP was added to a final concentration of 13 μM. Labelling was performed at 37 ºC on a roller drum for 20 min and all subsequent steps were done at RT. Cells were harvested by centrifugation at 16K RCF for 1 min and re-suspended in 100 μL of 3.7% formaldehyde in PBS for fixation. Cells were fixed for 10 min, harvested, and permeabilized using 100 μL of 0.5% Triton X-100 in PBS for 15 min. Cells were labelled using 100 μL of 1X Click-iT cocktail for 20 min in the dark. Cells were harvested and washed one time using Click-iT rinse buffer and then re-suspended in 20-40 μL of PBS for imaging or in 150 μL of PBS for fluorescence

measurement on a Tecan Infinite m200 plate reader in 96-well flat bottom White sided plates (Greiner Bio-One). Images were analyzed using Image J.

HPG labeling

Click-iT Plus HPG Alexa Fluor 488 Protein Synthesis Assay Kit (Invitrogen) was used to label cells with HPG following manufacturer's instructions. 450 μL of cells were transferred to disposable glass tubes. HPG was added to a final concentration of 60 μM. Labelling was performed at 37 ºC on a roller drum for 20 min and all subsequent steps were done at RT. Cells were harvested by centrifugation at 16K RCF for 1 min and re-suspended in 100 μL of 3.7% formaldehyde in PBS for fixation. Cells were fixed for 10 min, harvested, and permeabilized using 100 μL of 0.5% Triton X-100 in PBS for 15 min. Cells were labelled using 100 μL of 1X Click-iT cocktail for 20 min in the dark. Cells were harvested and washed one time using Click-iT rinse buffer and then re-suspended in 150 μL of PBS for fluorescence measurement on a Tecan Infinite m200 plate reader in 96-well flat bottom White sided plates (Greiner Bio-One).

Luminescence growth curves

Cultures were grown in LB from single colonies grown overnight at 37 ºC on LB plates. Cultures in exponential phase (OD_{600} ~ 0.5-1.0) were diluted to OD_{600} = 0.1 in 150 μL LB containing 4.7 mM D-luciferin (Goldbio) and grown in a 96-well flat bottom white sided plates (Greiner Bio-One) plates in triplicate. OD_{600} and luminescence measurements were made every five min using a Tecan Infinite m200 plate reader and media only wells were used to subtract background.

RNA quantification

RNA was quantified from cultures grown in LB as above. At given time points 14 mL of the cultures were pelleted at 8 K RCF for 10 minutes at room temperature and frozen at -80 ºC. Pellets were re-suspended in TRIzol (Invitrogen) to match based on OD_{600}. ~ 5 OD_{600} units of all cultures were

lysed using a FastPrep 24 5G (MP Biomedicals). Lysates were spun down at 20 K RCF for 20 min and RNA was extracted using the Direct-Zol RNA miniprep kit (Zymo Research). RNA samples were DNAse I treated following manufactures protocol (NEB) and 1 μg of RNA was used to generate cDNA using the High Capacity cDNA Reverse Transcription Kit (Applied Biosystems). cDNAs were diluted 1:200 and used as templates for qPCR. qPCRs were preformed using SYBR green. Primers were design using the PrimeQuest Tool (IDT). No cDNA and no RT controls were used to ensure signal was specific to desired RNAs.

***in vitro* translation assays**

Translation assays used the PURExpress system (NEB) following the manufacture's protocol and a plasmid encoding a CotE-FLAG fusion protein as template DNA (1). ppGpp (TriLink Biotechnologies) at the specified concentrations was added to translation reactions. Reactions were run for 20 min each at 37 ºC and stopped by adding 2X SDS loading buffer. Synthesized proteins were separated by SDS-PAGE, transferred to PVDF membranes and visualized by probing with an anti-FLAG HRP antibody (Sigma). Mutant IF2 was assayed using a ΔIF123 PURExpress kit (NEB) supplemented with equal concentrations of purified *E. coli* IF1 and IF3. Reactions were run essentially as above but 0.47 μM of either WT or mutant *B. subtilis* IF2 was added to each reaction as the sole source of IF2. WT and mutant IF2s were purified as previously described (2). Band intensities were analyzed using ImageJ.

DRaCALA binding assays

Radiolabeled (p)ppGpp was generated essentially as described (3). Briefly, purified *E. coli* RelA N-terminal mutant protein (amino acids 1-455) was incubated overnight at 30ºC with [α-^{32}P]- GTP (PerkinElmer) in 50 mM Tris (pH 8), 15 mM MgOAc, 60 mM KOAc, 30 mM NH4OAc, 0.2 mM EDTA, and 0.5 mM PMSF. Reactions were supplemented with 8 mM cold ATP. Conversion of GTP to (p)ppGpp (>90%) was monitored by thin layer chromatography on PEI-cellulose plates in

1.5 M KH2PO4 (pH 3.6). DRaCALA binding assays were carried out essentially as described (3, 4). 6 μM protein was incubated with 55.5 nM [α-^{32}P]-labeled (p)ppGpp in 40 mM Tris (pH 8), 100 mM NaCl, 10 mM $MgCl_2$, and 2mM PMSF. Reactions were incubated for 5 min at RT and 2.5 μL of each reaction was spotted onto nitrocellulose membranes and dried completely at RT. Spots were exposed for 30 min on a phosphor storage screen and visualized (GE Typhoon). Inner and outer ring intensities were quantified using ImageJ. Reactions where protein was not added were used to subtract background.

smFRET experiments

All of the *E. coli* components for assembling 30S ICs, including 30S ribosomal subunits, 5'-biotinylated mRNA, Cyanine (Cy) 3-labeled fMet-tRNA^{fMet} (labeled with maleimide-derivatized Cy3 at the naturally occurring 4-thiouridine at residue position 8), IF1, and Cy5-labeled IF2 (labeled with maleimide-derivatized Cy5 at an engineered cysteine at residue position 810) were prepared as previously described (5). 30S ICs lacking IF2 and IF3 were assembled by combining 0.6 μM 30S subunits, 1.8 μM 5'-biotinylated mRNA, 0.8 μM Cy3-labeled fMet-tRNA^{fMet}, and 0.9 μM IF1 in Tris-Polymix Buffer (50 mM Tris-OAc (pH_{RT} = 7.5), 100 mM KCl, 5 mM NH_4OAc, 5 mM $Mg(OAc)_2$, 0.1 mM EDTA, 5 mM putrescine-HCl, 1 mM spermidine-free base, and 6 mM β-mercaptoethanol). The reaction was incubated at 37 °C for 10 minutes then on ice for an additional 5 minutes. Small aliquots of 30S ICs were flash-frozen in liquid nitrogen and stored at -80 °C.

To conduct smFRET experiments, 30S ICs assembled were first diluted to a final concentration of 75 pM in the presence of 2 uM IF1, 25 nM Cy5-labeled IF2, and 1 mM GTP or ppGpp. 30S ICs were then tethered to the polyethylene glycol (PEG)/biotin-PEG-derivatized surface of a microfluidic observation flowcell using a biotin-streptavidin-biotin between the 5'-biotinylated mRNA and the biotin-PEG. Untethered 30S ICs were flushed from the flowcell, and tethered 30S ICs were buffer exchanged, by washing the flowcell with Imaging Buffer (Tris-Polymix Buffer with an oxygen scavenging system composed of 2.5 mM 3,4-dihydroxybenzoic

acid (PCA) and 250 mM protocatechuate 3,4-dioxygenase (PCD) and a triplet-state quencher cocktail composed of 8.4 mM 1,3,5,7-cyclooctatetraene (COT) and 8.7 mM 3-nitrobenzyl alcohol (NBA)) supplemented with 2 uM IF1, 25 nM Cy5-labeled IF2, and 1 mM GTP or ppGpp in order to enable rebinding of these components to 30SICs from which they might dissociates during the course of imaging. Finally, 30S ICs were imaged at single-molecule resolution and at a 0.1 sec per frame acquisition time using a laboratory-built, prism-based total internal reflection fluorescence (TIRF) microscope as previously described (5). A previously described approach (6) was used to identify fluorophores and classify them into 'fluorophore' or 'background' classes; align the Cy3 and Cy5 imaging channels; fit individual Cy3 and Cy5 fluorophore to 2D Gaussians and estimate and, in the case of Cy5, bleedthrough correct the Cy3 and Cy5 fluorescence emission intensity *versus* time trajectories; and generate the E_{FRET} *versus* time trajectories. Only those trajectories exhibiting a signal-to-background (SBR) of 3.5:1 or greater as well as single-step photobleaching of Cy3 within the observation time were selected for further analyses.

In order to estimate the rate constants for the association of IF2 with the 30S IC (k_a) and for the dissociation of IF2 from the 30S IC (k_d) we began by estimating a 'consensus' hidden Markov model (HMM) of the E_{FRET} *versus* time trajectories using a slight extension of the variational Bayes approach we introduced in the vbFRET algorithm (7). Briefly, instead of using a likelihood function for each E_{FRET} *versus* time trajectory, we used a single likelihood function that simultaneously includes all of the E_{FRET} *versus* time trajectories in a dataset to arrive at a log-likelihood function given by

$$\ln(\mathcal{L}) = \sum_{i \in trajectories} \ln(\mathcal{L}_i) \qquad \text{Eq. 1}$$

where $\mathcal{L}_i$ is the variational approximation of the likelihood function for a single trajectory. A further development of this approach in a hierarchical context underlies the hFRET algorithm that we have recently reported (8). Using this consensus HMM approach, we estimated HMMs for 1-6 states and performed model selection using the evidence lower bound (ELBO) as described in

Bronson et al., 2009. In all cases, the 2-state HMM was the model that yielded the highest ln(ELBO) or was the model with the fewest number of states of several models that yielded the highest ln(ELBO)s within < 2% of each other. The transition matrix obtained from this 2-state model consists of a 2 x 2 matrix in which the off-diagonal elements correspond to the number of times a transition takes place between the IF2-free and the IF2-bound states of the 30S IC and the on-diagonal elements correspond to the number of times a transition does not take place. From the transition matrix, transition probabilities (*p*) were calculated by dividing the number of transitions (i.e. off-diagonal elements) by the total number of times a state was observed (i.e. row sum of the transition matrix). These transition probabilities (*p*) were used to calculate rate constants (*k*) using the equation

$$k = -\frac{\ln(1-p)}{t}, \qquad \text{Eq. 2}$$

where *t* is the time between successive data points (*i.e.*, the acquisition time) (*t* = 0.1 sec). Subsequently, we calculated k_a using the equation

$$k_a = \frac{k'_a}{[IF2]}, \qquad \text{Eq. 3}$$

where k'_a is the pseudo-first-order association rate constant calculated using Eq. 2 and [IF2] is the concentration of IF2, and we calculated k_d directly using Eq 2. Using these values of k_a and k_d, we then calculated K_d using $K_d = k_d / k_a$.

As previously reported (6), the same transition matrix-based analysis described in the previous paragraph was used to correct for the effects of Cy5 photobleaching in E_{FRET} *versus* time trajectories for IF2(GTP). Briefly, the relatively high stability of the IF2-bound state for IF2(GTP) results in a situation in which IF2(GTP) can remain stably bound to the 30S IC after Cy5 photobleached. Consequently, failure to account for the effect of Cy5 photobleaching in E_{FRET} *versus* time trajectories for IF2(GTP) can result in an overestimation of k_d. Thus, in order to correct for the effect of Cy5 photobleaching, the final dwell of the IF2-bound state for each E_{FRET} *versus* time trajectory for IF2(GTP) was not included in our calculation of k_d.

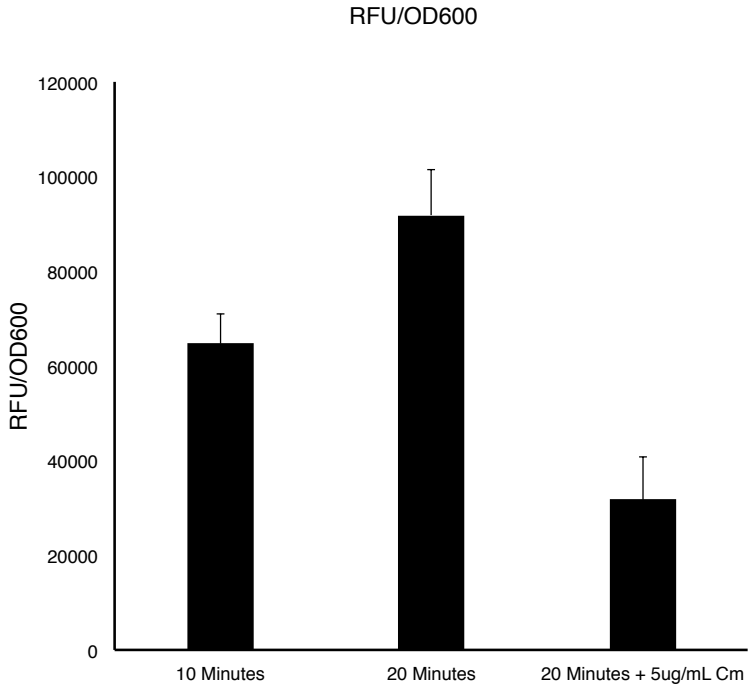

Figure S1. OPP does not arrest protein synthesis

The effect of OPP addition on protein synthesis was tested during exponential phase. OPP was added to exponentially growing cultures of WT *B. subtilis* and total fluorescence was measured at 10 minutes and 20 minutes post OPP addition. Increased fluorescence was detected at the 20 minute time point compared to 10 minute time point indicating continued protein synthesis in the presence of OPP. Chloramphenicol was added to a separate culture in combination with OPP. Decreased fluorescence indicates that OPP is sensitive to translational inhibition (means ± SDs).

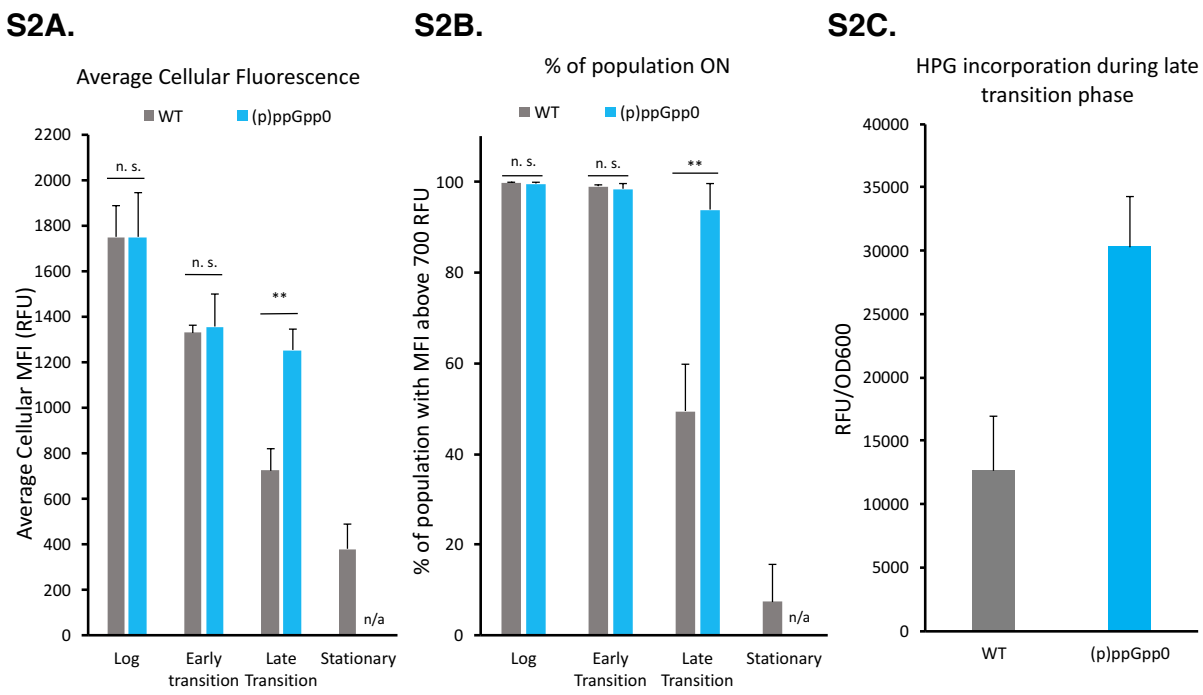

Figure S2. Supplementary data for Figure 1

(A) Average cell fluorescence and **(B)** % of population ON were quantified from ~1400 cells in three separate experiments (means ± SDs). **(C)** HPG incorporation for WT and (p)ppGpp^0 strains during transition phase (means ± SDs) n.s. $p > 0.05$, *$p < 0.05$, **$p < 0.01$, ***$p < 0.001$

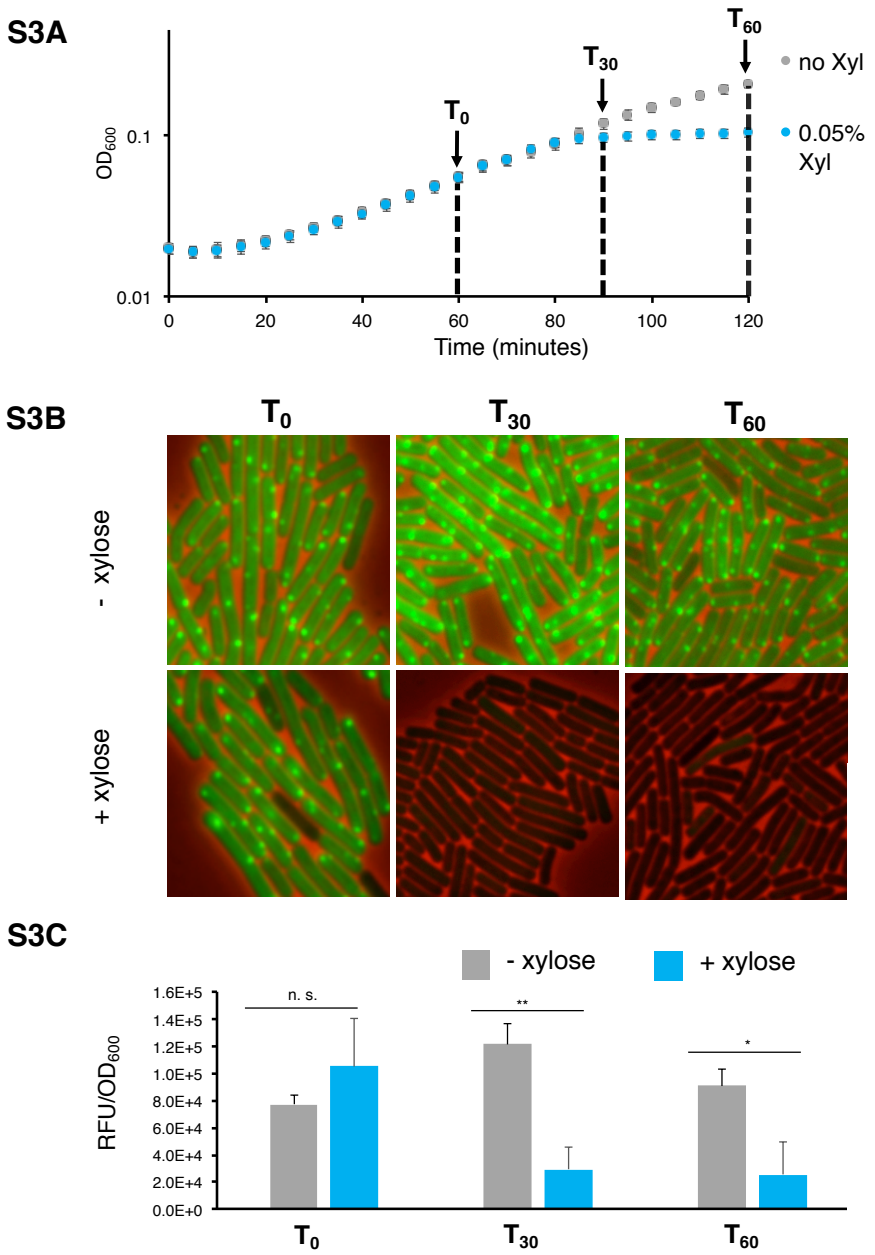

Figure S3. (p)ppGpp is sufficient to inhibit growth and protein synthesis

SasA was expressed during exponential phase growth and cells were labelled with OPP. (A) A P_{xyl}-*sasA* strain (JDB 4295) was grown in duplicate and 0.05% xylose was added after 60 min of growth (T_0) and growth was monitored for 60 min post induction (means ± SDs). (B) Representative pictures of OPP-labelled induced and un-induced cultures of P_{xyl}-*sasA* strain at time points post induction. (C) Total fluorescence of OPP labelled induced and un-induced cultures of P_{xyl}-*sasA* strain at different time points post induction. Time points in (B) and (C) are designated by black dashed lines in (A) (means ± SDs). n.s. $p > 0.05$, *$p < 0.05$, **$p < 0.01$, ***$p < 0.001$

S4A.

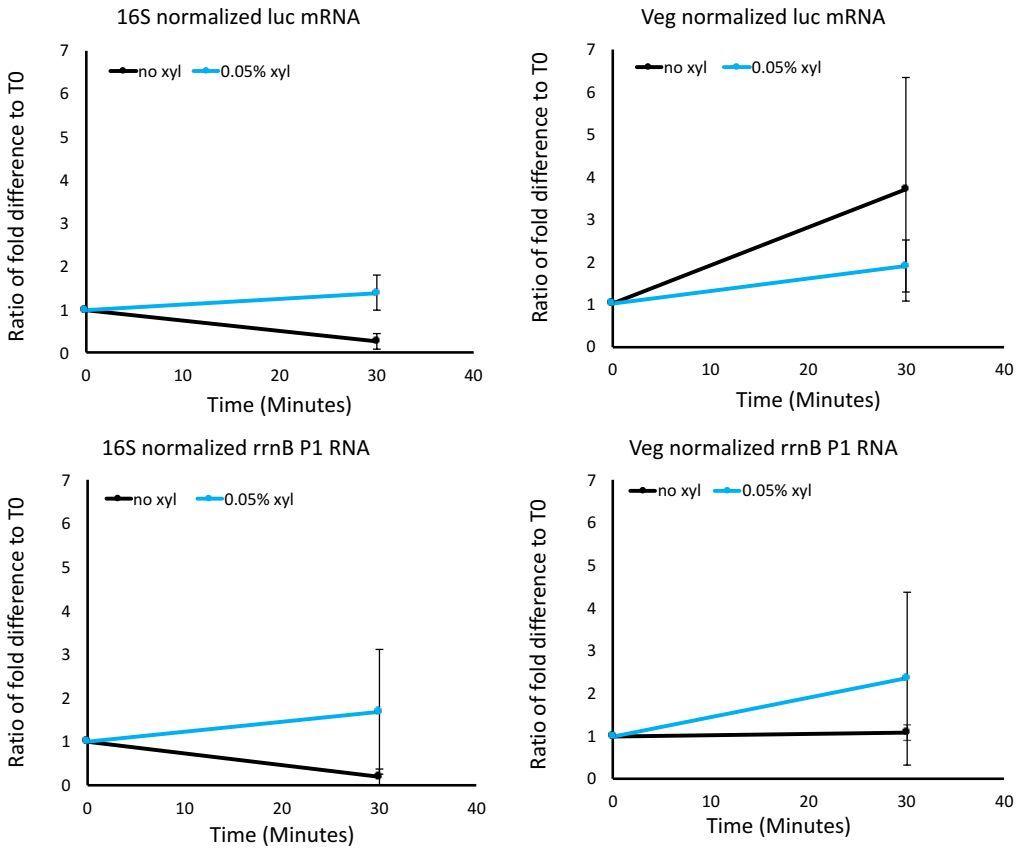

S4B.

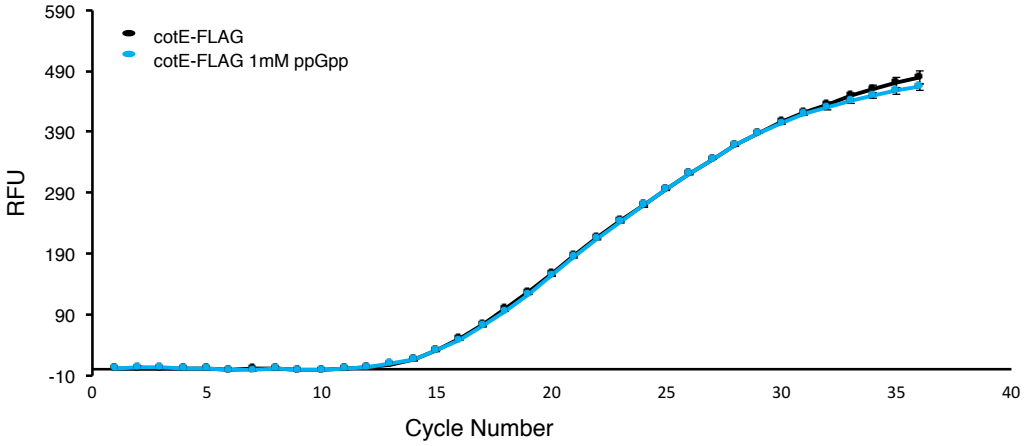

Figure S4. (p)ppGpp inhibits translation specifically in Fig 2.
(A) Direct inhibition of translation of the luciferase reporter by (p)ppGpp was verified by measuring *luc* mRNA and *rrnB* P1 rRNA (as a measure of GTP concentration) both at the time of induction and a time point when the *luc* reporter was significantly inhibited (T_0 and T_{30} respectively) using RT-qPCR. We observed no statistically significant decrease in luc mRNA or rrnB P1 rRNA between the un-induced or induced cultures using either the mature 16S rRNA or the veg gene mRNA as a housekeeping gene (means ± SEMs). **(B)** Synthesis of *in vitro* transcribed *cotE* mRNA was measured by quantifying total mRNA produced in the presence of a concentration of ppGpp (1mM) that significantly inhibits protein production. RNA was quantified using RT-qPCR

(means ± SDs). Compare with 1mM concentration in Figure 2. n.s. $p > 0.05$, *$p < 0.05$, **$p < 0.01$, ***$p < 0.001$.

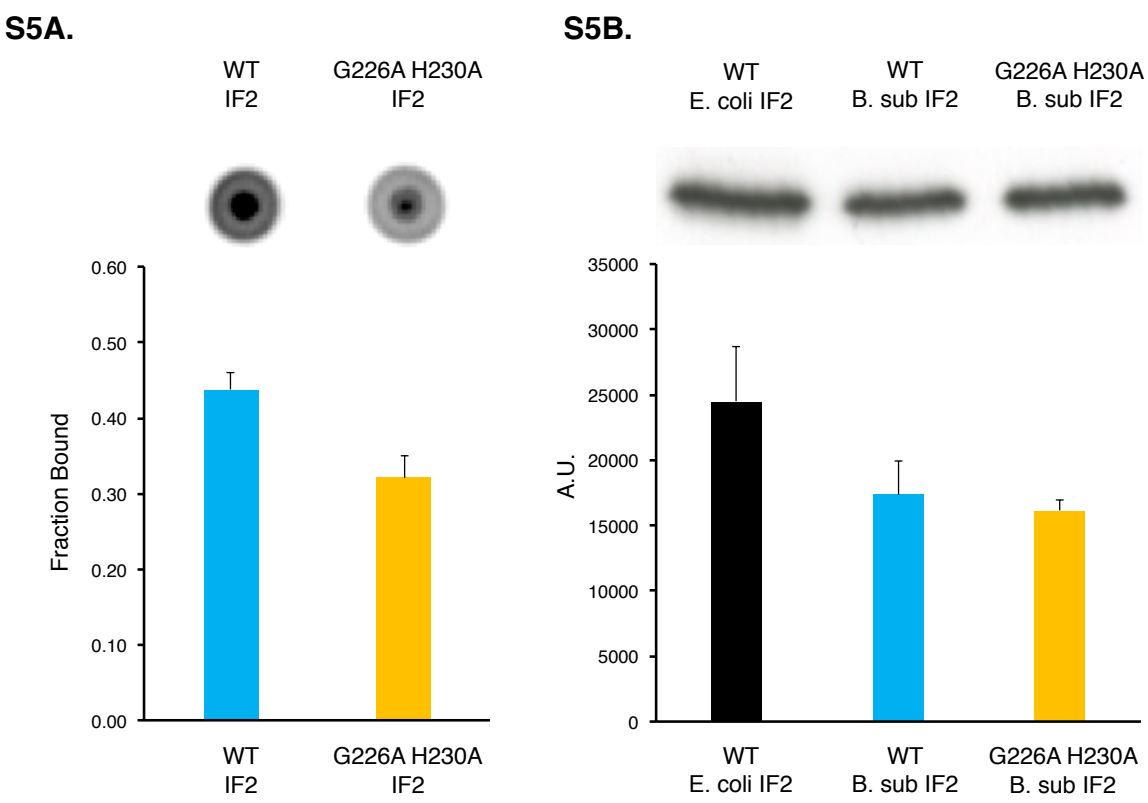

Figure S5. G226A H230A IF2 mutant is inhibited in binding GTP but not in function
(A) GTP binding and **(B)** function of G226A H230A IF2 mutant was assayed using DRaCALA assay and an *in vitro* transcription-translation assay respectively (means ± SDs).

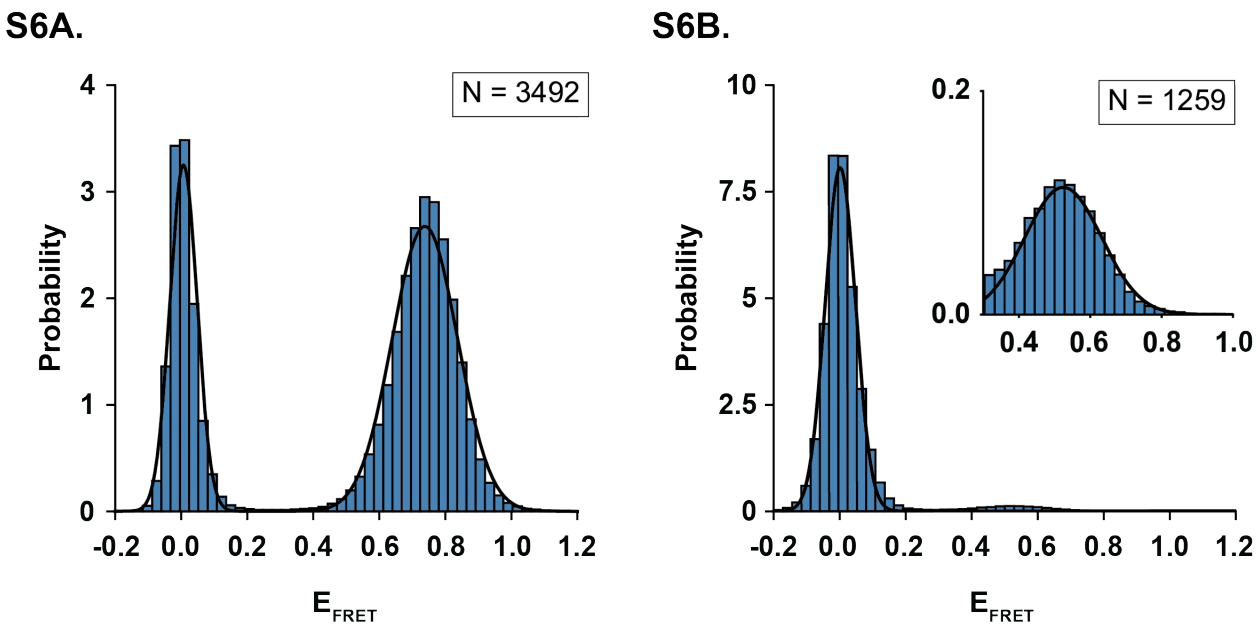

Figure S6. IF2(GTP) and IF2(ppGpp) exhibit distinct conformations when bound to the 30S IC

One-dimensional histograms of E_{FRET} value distributions corresponding to the interaction of IF2 with the 30S IC for **(A)** IF2(GTP) and **(B**) IF2(ppGpp). Both histograms were fitted to a two-Gaussian mixture model in which the Gaussian centered at the zero E_{FRET} value corresponds to the IF2-free state of the 30S IC and the Gaussian centered at the non-zero E_{FRET} value corresponds to the IF2-bound state of the 30S IC. However, for the histogram corresponding to IF2(ppGpp), the IF2-bound state was re-fitted to a single Gaussian for datapoints in which E_{FRET} > 0.2 (inset). The center of each fitted Gaussian was used to determine the mean E_{FRET} value for the corresponding state ($\langle E_{FRET} \rangle$). The Gaussians corresponding to the IF2-free, IF2(GTP)-bound, and IF2(ppGpp)-bound states of the 30S IC had $\langle E_{FRET} \rangle$s of ~0.0 (in both histograms), ~0.74, and ~0.53, respectively.

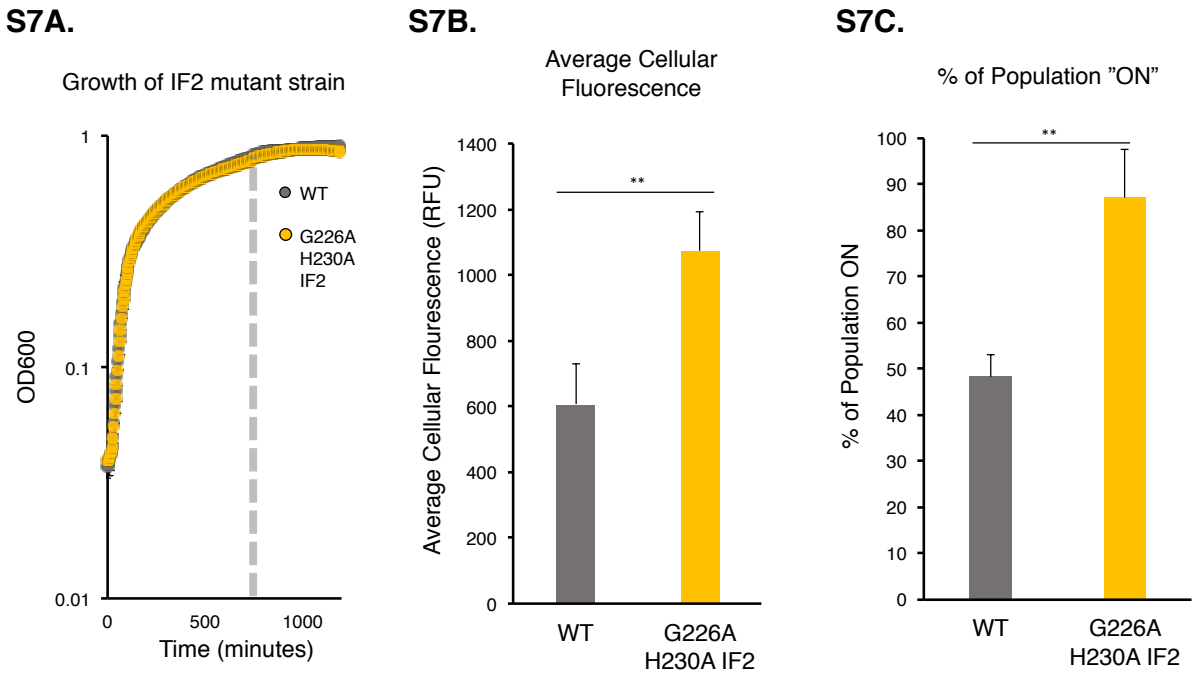

Figure S7 Growth curve average cellular fluorescence and % of population ON throughout growth in WT and G226A H230A *infB* strains

(A) Growth curve of G226A H230A IF2 strain is equivalent to WT. **(B)** Average cell fluorescence and **(C)** % of population ON were quantified from ~1400 cells in three separate experiments (means ± SDs). n.s. $p > 0.05$, *$p < 0.05$, **$p < 0.01$, ***$p < 0.001$

Supplementary Tables

Table S1. Association rate constant (k_a), dissociation rate constant (k_d), and equilibrium dissociation constant (K_d) for the interaction of IF2(GTP) and IF2(ppGpp) with the 30S IC.

	k_a (μM^{-1} s^{-1})[a]	k_d (s^{-1})[a]	K_d (nM)[a]
IF2(GTP)	4.9 ± 0.2	0.032 ± 0.003[b]	6.5 ± 0.2
IF2(ppGpp)	3.3 ± 0.3	2.0 ± 0.3	616 ± 140

[a] k_a, k_d, and K_d were obtained from three independently collected datasets (mean ± SE)

[b] k_d was corrected for the effects of Cy5 photobleaching as described in Methods

Table S2. Plasmids used in this study

pDR150		
pVEG		
pGL3		
pSac-cm		
pMINIMAD2		
pETPHOS		
pDR150 *ywaC*	This study	pSD49
pSac-cm-P_{veg}-*luc*	This study	pSD47
pMINIMAD2 *G226A H230A B. subtilis infB*	This study	pSD54
pETPHOS *B. subtilis infB*	This study	pSD36
pETPHOS *G226A H230A B. subtilis infB*	This study	pSD53
pETPHOS *B. subtilis fusA*	This study	pSD30
pETPHOS *E.coli 1-455 relA*	This study	pSD56

Table S3. Strains used in this study

168 trpC2 (WT)	Lab stock	JDB 1772
trpC2 ΔywaC::kan ΔyjbM::tet ΔrelA::erm	(9)	JDB 4294
trpC2 amyE:P_{xyl}-ywaC spc ΔywaC::kan ΔyjbM::tet ΔrelA::erm	This study	JDB 4295
trpC2 sacA:P_{veg}-luc cm amyE:P_{xyl}-ywaC spc ΔywaC::kan ΔyjbM::tet ΔrelA::erm	This study	JDB 4296
trpC2 G226A H230A infB	This study	JDB 4297
MG1655	Lab stock	JDE 1497
BL21 pETPHOS pSD36	This study	JDE 3077
BL21 pETPHOS pSD53	This study	JDE 3078
BL21 pETPHOS pSD30	This study	JDE 3075

BL21 pETPHOS pSD56	This study	JDE 3079

Table S4. Oligonucleotides used in this study

GGAAGTCGACAAGGAGGGCGAAAAATGGATTTATCTGTAACACATA	This study	*ywaC* RBS SalI F
CCCAAAGGATCCTTAATCCACTTCTTTCTTAATC	This study	*ywaC* BamHI R
GATCGGATCCGCGGCCGCTTCTAGAGGGAGTTCTGAGAATTGGTATGC	This study	P_{veg} BamHI F
GATCAAGCTTAACTACATTTATTGTACAACACGAGC	This study	P_{veg} HindIII R
GGGAAAAAGCTTGGCATTCCGGTACTGTAGGAGGAGCCACCATGGAAGACGC	This study	*luc* RBS HindIII F
AAAGGGGAATTCGAATTACACGGCGATCTT	This study	*luc* R EcoRI
GGGAAAGAATTCATGGCTAAAATGAGAGTATACG	This study	*infB* EcoRI F
GGGAAAGGATCCATTCAAACCGGTAATTTCAACC	This study	*infB* BamHI R
GACAATCATGGCTCACGTTGACC	This study	*infB* G226A F
GGTCAACGTGAGCCATGATTGTC	This study	*infB* G226A R
CCACGTTGACGCTGGGAAAACAA	This study	*infB* H230A F
TTGTTTTCCCAGCGTCAACGTGG	This study	*infB* H230A R
GGGAAACATATGGCTAAAATGAGAGTATACG	This study	*infB* NdeI F
GGGAAAGGATCCGCAAATCCGATCACGTTCTTTCAATTTCTTGC	This study	*infB* BamHI R
GGAAGTCGACAAGGAGGGCGAAAAATGGATTTATCTGTAACACATA	This study	*fusA* NdeI F
CCCAAAGGATCCTTAATCCACTTCTTTCTTAATC	This study	*fusA* BamHI R
GATCGGATCCGCGGCCGCTTCTAGAGGGAGTTCTGAGAATTGGTATGC	This study	*E. coli relA* NdeI F
GATCAAGCTTAACTACATTTATTGTACAACACGAGC	This study	*E. coli relA* N-terminal domain R BamHI

SI References

1. Pereira SF, Gonzalez RL, Jr., & Dworkin J (2015) Protein synthesis during cellular quiescence is inhibited by phosphorylation of a translational elongation factor. *Proc Natl Acad Sci U S A* 112(25):E3274-3281.
2. Fei J*, et al.* (2010) A Highly Purified, Fluorescently Labeled In Vitro Translation System for Single-Molecule Studies of Protein Synthesis. *Single Molecule Tools: Fluorescence Based Approaches, Part A,* Methods in Enzymology), pp 221-259.
3. Corrigan RM, Bellows LE, Wood A, & Grundling A (2016) ppGpp negatively impacts ribosome assembly affecting growth and antimicrobial tolerance in Gram-positive bacteria. *Proc Natl Acad Sci U S A* 113(12):E1710-1719.

4. Roelofs KG, Wang J, Sintim HO, & Lee VT (2011) Differential radial capillary action of ligand assay for high-throughput detection of protein-metabolite interactions. *Proc Natl Acad Sci U S A* 108(37):15528-15533.
5. Caban K, Pavlov M, Ehrenberg M, & Gonzalez RL, Jr. (2017) A conformational switch in initiation factor 2 controls the fidelity of translation initiation in bacteria. *Nat Commun* 8(1):1475.
6. Desai BJ & Gonzalez RL (2019) Multiplexed, bioorthogonal labeling of multicomponent, biomolecular complexes using genomically encoded, non-canonical amino acids. *bioRxiv*.
7. Bronson JE, Fei J, Hofman JM, Gonzalez RL, Jr., & Wiggins CH (2009) Learning rates and states from biophysical time series: a Bayesian approach to model selection and single-molecule FRET data. *Biophys J* 97(12):3196-3205.
8. Hon J & Gonzalez RL, Jr. (2019) Bayesian-Estimated Hierarchical HMMs Enable Robust Analysis of Single-Molecule Kinetic Heterogeneity. *Biophys J* 116(10):1790-1802.
9. Mirouze N, Prepiak P, & Dubnau D (2011) Fluctuations in spo0A transcription control rare developmental transitions in Bacillus subtilis. *PLoS Genet* 7(4):e1002048.